

Article

Prediction of Oxygen Distribution in Silos and Chambers Filled with Various Agricultural Commodities

Efstathios Kaloudis ^{1,*}, Paraskevi Agrafioti ² and Christos Athanassiou ²

¹ Computer Simulation, Genomics and Data Analysis Laboratory, Department of Food Science and Nutrition, School of the Environment, University of the Aegean, 81400 Lemnos, Greece

² Laboratory of Entomology and Agricultural Zoology, Department of Agriculture, Crop Production and Rural Environment, University of Thessaly, 38446 Volos, Greece; agrafiot@uth.gr (P.A.); athanassiou@uth.gr (C.A.)

* Correspondence: stathiskaloudis@aegean.gr

Abstract: In the context of post-harvest pest management in agricultural products, the adoption of modified atmospheres presents an eco-friendly alternative to conventional pesticides. This study focuses on nitrogen gas as a potential agent for insect control in stored commodities, utilizing computational simulations (by employing the convection–diffusion equation) to investigate its penetration and distribution within two common storage configurations: chamber-contained pallets and silos. The results highlight the influence of boundary conditions, commodity porosity, and convection effects on nitrogen dispersion. In chamber scenarios, the first boundary condition considers that pallets are placed inside a chamber with uniform (99.5%) nitrogen concentration, whereas in the second one, the concentration gradually increases from 78% to 99.5%. The average duration required for O₂ concentration to reach 1% is approximately 10.7 h and 133.3 h for the two boundary conditions, respectively. Among the agricultural commodities, walnuts (kernels) exhibit the shortest duration, while prunes require the longest time. In silos, convection and diffusion interact to establish a consistent diffusion layer thickness. Most agricultural products exhibit similar behavior, with average times of 13.5 h, 25.4 h, and 37.0 h for three heights (10 m, 20 m, and at the silo's top at 30 m), respectively.

Keywords: numerical modeling; simulation; nitrogen; modified atmospheres; low oxygen



Citation: Kaloudis, E.; Agrafioti, P.; Athanassiou, C. Prediction of Oxygen Distribution in Silos and Chambers Filled with Various Agricultural Commodities. *Agronomy* **2023**, *13*, 3027. <https://doi.org/10.3390/agronomy13123027>

Academic Editor: Milena Petriccione

Received: 30 September 2023

Revised: 29 November 2023

Accepted: 5 December 2023

Published: 10 December 2023



Copyright: © 2023 by the authors. Licensee MDPI, Basel, Switzerland. This article is an open access article distributed under the terms and conditions of the Creative Commons Attribution (CC BY) license (<https://creativecommons.org/licenses/by/4.0/>).

1. Introduction

Modified atmospheres offer a promising approach for effectively managing insects in post-harvest stages of agricultural products, serving as a viable alternative to conventional pesticides. With growing concerns among consumers about the hazards associated with residual insecticides in food and their detrimental impact on the environment, adopting modified atmospheres on an industrial scale presents a feasible and eco-friendly strategy for pest control across various commodities [1–3]. The term ‘modified atmospheres’ encompasses a range of techniques aimed at altering gas proportions within a designated space, such as a chamber. This adjustment involves introducing specific gases, like nitrogen or carbon dioxide, to significantly reduce oxygen levels or elevate carbon dioxide concentrations. This deliberate atmospheric manipulation capitalizes on the fact that insects and many microorganisms rely on oxygen for their aerobic processes. Consequently, modifying the atmosphere can severely impede their development and ultimately jeopardize their survival [3].

The advantages of using modified and controlled atmospheres for disinfestation are multifaceted. First and foremost, these techniques are environmentally friendly and minimize the use of chemical pesticides, reducing the risk of pesticide residues in stored products. This aligns with the growing consumer demand for safer and more sustainable agricultural practices. Furthermore, modified and controlled atmospheres are non-toxic to humans and do not pose health risks to workers or consumers. They also do not contribute to the development of pesticide resistance in pests, which is a significant concern

with traditional chemical treatments. As a result, these methods can be integrated into an integrated pest management (IPM) strategy, promoting long-term pest control and reducing the need for repeated treatments [4].

Prior investigations into nitrogen utilization have exhibited encouraging outcomes against numerous insect species prevalent in stored products. For example, Ofuya and Reichmuth [5] systematically examined the impact of a nitrogen atmosphere comprising 100% concentration on all life stages of the cowpea weevil, *Callosobruchus maculatus* (F.) (Coleoptera: Bruchidae), as well as the bean weevil, *Acanthoscelides obtectus* (Say) (Coleoptera: Bruchidae). Their findings indicated a 100% mortality rate within exposure intervals ranging from 1 to 9 days. Furthermore, earlier research has demonstrated the survival capabilities of stored-product insects under exceedingly low oxygen concentrations, persisting for extended periods, spanning days or even weeks. This has led to the proposal that the necessary oxygen levels for achieving a desirable degree of insect control should remain below 2% [6]. Within the scope of this investigation, the impact of nitrogen, administered as a controlled atmosphere treatment, on the microbial and entomological loads, as well as the organoleptic characteristics of stored dried currants (Corinthian raisins, *Vitis vinifera* L. var. *Apyrena*), was investigated. Experimental trials were executed under realistic conditions within the nitrogen chambers of a commercial facility, wherein nitrogen was introduced through an integrated nitrogen generator. Despite discernible effects on taste, odor, aroma, and overall acceptance attributable to the applied treatments, the sensory attributes of Corinthian currants remained within acceptable parameters subsequent to nitrogen fumigation. Recently, Rumbos et al. [7] tested nitrogen treatment (>99%) on a commercial scale to control major stored product insects such as the rice weevil, *Sitophilus oryzae* (L.) (Coleoptera: Curculionidae), the lesser grain borer, *Rhyzopertha dominica* (F.) (Coleoptera: Bostrychidae), the larger grain borer, *Prostephanus truncatus* (Horn) (Coleoptera: Bostrychidae), the confused flour beetle, *Tribolium confusum* Jacquelin du Val (Coleoptera: Tenebrionidae), and the sawtoothed grain beetle, *Oryzaephilus surinamensis* (Coleoptera: Silvanidae), and found that nitrogen treatment is effective for all life stages and populations tested.

Despite the promise of utilizing modified atmospheres with nitrogen, and the increasing number of studies in the scientific literature, there exists insufficient information regarding the penetration of nitrogen into packaged goods such as pallets or vertical structures like silos. Acquiring experimental data can be challenging and resource-intensive in terms of time and cost. Conversely, numerical investigations offer a viable approach, enabling storage managers and practitioners to enhance their comprehension of the fundamental mechanisms governing nitrogen diffusion in diverse storage environments and agricultural commodities. Within this context, numerical modeling has been partially employed in analogous applications. Specifically, Agrafioti et al. [8] published a study concerning the practical application of modified atmospheres to combat phosphine-resistant insect populations in commercial settings. Specifically, they assessed the efficacy of this method against two predominant species of stored-product beetles, *R. dominica* and *O. surinamensis*. These evaluations were conducted within commercial facilities where they introduced nitrogen through a nitrogen generator. Each testing chamber accommodated three to four pallets laden with either currants or herbs. To analyze nitrogen concentration, they developed a computational model. The computational model operated under the assumptions that nitrogen concentration in proximity to the pallets remains uniform and that the primary mechanism governing nitrogen dispersion within the pallet is gas diffusion. To this end, the model solved the diffusion equation. Across the majority of trials, they consistently recorded 100% mortality rates for both beetle species, encompassing all tested temperature conditions and exposure durations. In terms of control progeny production, *R. dominica* exhibited a range between 20 and 45 adults per vial, while *O. surinamensis* displayed a range from 29 to 27 adults per vial. The simulation results demonstrate that nitrogen can efficiently permeate currants, with negligible differences in concentration (less than 1.5%) observed across the pallet. Furthermore, the simulation model elucidated that lower temperatures do not significantly impact nitrogen concentration profiles.

The study by Guo et al. [9] presents numerical simulation findings involving liquid nitrogen injection into a container, indicating the efficacy and applicability of controlled atmosphere treatments for preserving mature pepino fruit quality. Specifically, it investigated the influence of recirculation velocity on the oxygen volume fraction and temperature distribution within a controlled atmosphere container through the introduction of liquid nitrogen. A three-dimensional (3D) model was formulated, and numerical simulations were employed to elucidate the airflow, heat transfer, and mass transfer dynamics associated with liquid nitrogen injection. To validate the model's accuracy, a validation test was conducted. The outcomes of this investigation reveal that augmenting recirculation velocity prolongs the duration of liquid nitrogen injection while concurrently diminishing temperature differentials within the container and on the surfaces of fruits and vegetables. In their simulations, the equations governing mass, momentum, and heat transfer were solved using the finite volume method, along with their corresponding boundary conditions. A tetra/mixed mesh configuration was chosen to discretize the computational domain into numerous small elements. Within each element, the three velocity components, pressure, and temperature were approximated through the employment of the finite volume method, wherein all pertinent parameters were computed using discretization equations subsequent to integration. Mesh refinement was applied strategically, focusing on regions such as the fan outlet, vaporizing coil outlet, and exhaust valve, to enhance simulation accuracy in these specific components.

Silva et al. [10] conducted an investigation and employed a computational fluid dynamics (CFD) model to elucidate the dynamics of ozone gas flow within an aeration system, specifically targeting a lethal concentration for the maize weevil, *Sitophilus zeamais* Motschulsky (Coleoptera: Curculionidae), in rice grains. Utilizing the CFD technique, they modeled the gas flow and adjusted the model to experimental data by considering critical parameters such as the mass transfer coefficient and the ozone–rice grain reaction constant. Subsequently, they conducted a simulation involving the injection of ozone gas into a silo with a static capacity of 69.6 tons of rice. To model the flow of ozone gas through the column of rice grains, Silva et al. [10] utilized the ANSYS CFX V11.0 software for CFD analysis. Computational meshes were generated using CFX Mesh, with a mesh comprising 8840 nodes and a temporal resolution set at 6 h following a thorough spatial and temporal convergence assessment. The gas within the intergranular spaces was assumed to be an ideal mixture of air and ozone gas. We considered the flow to be laminar, incompressible, isothermal, and transient in both simulated scenarios, justified by the low Reynolds number characterizing the flow regime. The governing equations for the porous medium encompassed the Navier–Stokes equations and transport equations governing ozone gas within both the gaseous and solid phases. Similarly, Carvalho et al. [11] also explored nitrogen gas concentration for refrigeration and atmosphere adjustment in corn storage. Furthermore, Pandiselvam et al. [12] employed numerical simulations to predict ozone concentration and flow characteristics in bulked paddy rice. Agrafioti et al. [13] utilized CFD to model phosphine gas distribution within grain silos and metal containers, successfully validating this model in a real-world scenario.

In light of the above, it becomes apparent that there is a scarcity of scientific investigations and computational models dedicated to simulating the distribution of nitrogen and oxygen during controlled atmosphere treatments. Additionally, experimental inquiries have thus far addressed only a limited array of configurations for various storage spaces and agricultural commodities. Given the expansive potential combinations, it necessitates substantial effort to comprehensively cover them experimentally. Consequently, the focus of the present study is directed towards the development of a computational model. This model aims to explore the penetration and distribution patterns of nitrogen and oxygen within two prevalent storage configurations for agricultural products: chamber-contained pallets and silos. Moreover, the study addresses a diverse range of commonly treated agricultural products in its simulations, thereby providing practitioners with valuable insights into these applications.

2. Materials and Methods

2.1. Computational Model Description

The convection–diffusion, or advection–diffusion, equation serves as a fundamental tool for elucidating transport phenomena involving the transfer of heat, mass, and other physical properties through diffusion and advection mechanisms [14]. In the context of a one-dimensional spatial domain devoid of sources or sinks, and with constant diffusivity (D_{eff}) and velocity (u), the convection–diffusion equation is succinctly expressed as follows:

$$\frac{\partial C}{\partial t} + u \frac{\partial C}{\partial x} = D_{eff} \frac{\partial^2 C}{\partial x^2} \quad (1)$$

where the variable C represents the concentration (%) of nitrogen gas, while t denotes the temporal parameter in seconds (s) and x denotes the spatial parameter measured in meters (m). The symbol D_{eff} corresponds to the effective diffusion coefficient with units of m^2/s , which accommodates porous effects inherent to gas flow within the product matrix. The solution to Equation (1) provides predictions regarding nitrogen (and consequently, oxygen) concentration during controlled atmosphere treatments, be it within silos or chamber-contained pallets. For the latter scenario, we posit a uniform nitrogen concentration encompassing the pallets (in adherence to a Dirichlet boundary condition), where gas diffusion predominates ($u = 0$ m/s) as the chief modality for nitrogen gas dispersion within the pallet structure. The numerical simulations are executed upon a one-dimensional mesh framework, thereby yielding predictions concerning the spatial separation between the chamber's concentration domain (exterior surface of the pallet) and the pallet's core. In the context of silos, these simulations extend to the vertical gap spanning from the silo's base to its apex.

According to Shen and Chen [15], in order to represent the role of porosity (ϕ) on ordinary molecular diffusion, the diffusion coefficient (D_m [m^2/s]) must be scaled with tortuosity (τ). Porosity is a dimensionless parameter and is equal to the ratio of pore volume to total volume [14]. Tortuosity is a dimensionless parameter as well, which can be defined as the ratio of average length of the geometric flow paths through the porous medium to the straight-line length across the porous medium [16]. Based on the above, an effective diffusivity coefficient could be set as:

$$D_{eff} = \frac{D_m}{\tau^2} \quad (2)$$

Shen and Chen [15], in their review article, studied numerous formulations of porosity in a system of porous media. A relation between tortuosity and porosity for random homogeneous isotropic sphere packings [17] is provided by the equation:

$$\tau^2 = \frac{3 - \phi}{2} \quad (3)$$

The temperature-dependent binary diffusion coefficient (D_m [m^2/s]) for nitrogen and oxygen is calculated based on the equation provided by Bird et al. [14]:

$$D_m = 1.859 \times 10^{-6} \frac{T^{\frac{3}{2}}}{p \sigma_{12}^2 \Omega} \sqrt{\frac{1}{MW_1} + \frac{1}{MW_2}} \quad (4)$$

where T is the absolute temperature [K], MW is the molar mass [g/mol], p is the pressure [atm], $\sigma_{12} = \frac{1}{2}(\sigma_1 + \sigma_2)$ is the average collision diameter (Å), 1 and 2 index the two kinds of molecules present in the gaseous mixture, and Ω is the collision integral (dimensionless). The values of Ω and σ_{12} are temperature-dependent and can be computed with the assistant of the corresponding tables found in the literature [14]. For the present study, the temperature dependence of D_m was calculated based on the above and the results are shown in Figure 1. Indicatively, D_m is equal to $1.944 \times 10^{-5} m^2/s$ and $2.064 \times 10^{-5} m^2/s$ at temperatures 20 [°C] and 30 [°C], respectively.

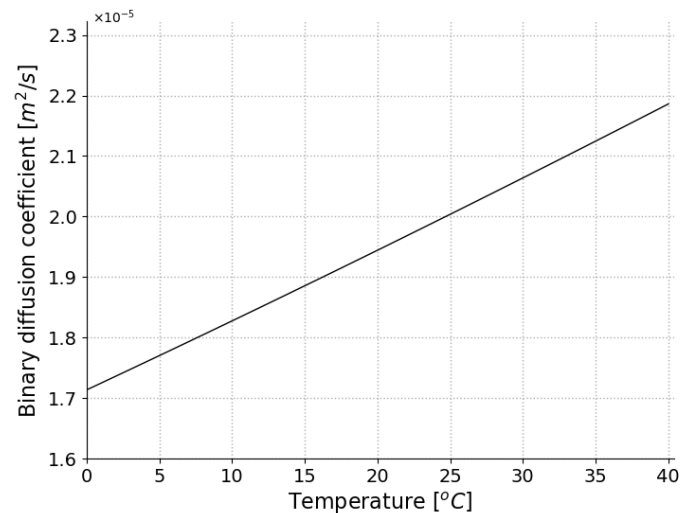


Figure 1. The dependence in temperature of the binary diffusion coefficient (D_m).

In summary, given the availability of porosity values, the complete set of parameters is established, enabling the utilization of Equation (1) for predictive purposes. The pertinent porosity values for a selection of prevalent commodities that undergo nitrogen treatments are tabulated in Table 1.

Table 1. Porosity values per commodity.

Product	Porosity	Source
almonds (in-hull)	0.67	[18]
almonds (in-shell)	0.58	[18]
barley	0.45	[19]
cashew	0.49	[20]
corn	0.48	[21]
hazelnut (kernel)	0.43	[22]
pistachio (nut)	0.57	[23]
pistachio (kernel)	0.50	[23]
prunes	0.33	[24]
raisins	0.40	[25]
rice	0.57	[26]
soy bean	0.38	[27]
walnut (shelled)	0.61	[28]
walnut (kernel)	0.75	[28]
wheat	0.44	[29]

2.2. Validation

To evaluate the precision of the computational code, the authors validated the model predictions against both the numerical solution presented by Zoppou and Knight [30] and experimental data available in the scientific literature [31]. As previously mentioned, Zoppou and Knight [30] provided the numerical solution for Equation (1),

$$C(x, t) = \frac{C_o}{2} \operatorname{erfc} \left[\frac{x - ut}{2\sqrt{D_{eff}t}} \right] + \frac{C_o}{2} \exp \left[\frac{ux}{D_{eff}} \right] \operatorname{erfc} \left[\frac{x + ut}{2\sqrt{D_{eff}t}} \right] \quad (5)$$

The authors compared the model results with the solution provided by Zoppou and Knight [30] (Equation (5)) when $u = 1$ [$m\ s^{-1}$], $D_{eff} = 0.02$ [m^2s^{-1}], $C_o = 100$ [%] at $t = 2$ [s]. The results are shown in Figure 2. It is evident that the model accurately solves the equation, aligning closely with the numerical solution. Notably, the Mean Absolute Error was calculated to be 0.02987.

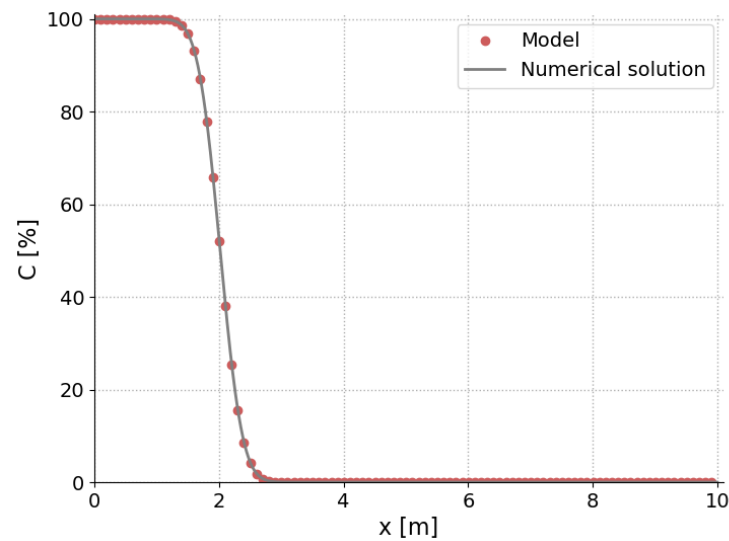


Figure 2. Comparison of the spatial (x) dependence of the model results on gas concentration (C) with the analytical solution.

To access further the accuracy of the model, we ran simulations for a nitrogen application as described by Navarro et al. [31]. Navarro et al. [31] reported a nitrogen application to a concrete silo containing 2400 tonnes of wheat at the Cyprus Grain Commission's Limassol port silo. The silo, constructed from concrete (with a bin diameter of 10.5 m, eaves height of 33.4 m, and a total storage capacity of 3046 m³), underwent structural sealing procedures, alongside the installation of air-tight valves, to increase bin gas tightness. The bin received a grain load, reaching approximately 1 m below the bin roof, containing 2400 tonnes of wheat (with moisture content at 11.8% on a wet basis, and temperature at 19 °C). Oxygen (O₂) levels were monitored through gas sampling at heights 1 m above and 3 m below the grain surface, followed by analysis via a portable meter. Upon achieving an O₂ concentration below 0.9% within the bin, this concentration was persistently upheld through the EcO₂ system, ensuring it remained below 0.9%. The employed EcO₂ generator utilized pressure swing adsorption (PSA) technology for air-to-N₂ production. This system was integrated into a mobile 6 m container, complete with essential equipment and control devices. A flexible tube (25 mm internal diameter) at the bottom of the silo was used to fill the silo bin with N₂ from the EcO₂ generator. Purge time was 56 h until 0.9% O₂ concentration was reached and the nitrogen volume used to reach this concentration was 3571 m³. Based on the above data, the model predicts that the 0.9% O₂ concentration will be reached after 53.97 h, which is very accurate since it differs 3.62% from the duration (56 h) reported by Navarro et al. [31].

3. Results

3.1. Chamber

The objective of this section is to provide an approximate rule of thumb duration for achieving a 1.0% O₂ concentration at the center of a pallet during a nitrogen treatment for a wide range of agricultural products. While there is no single standardized pallet dimension, several different sizes are commonly used. According to the ISO 6780 standard [32], the largest dimension of a pallet is 1.219 m.

For the purposes of this section, two different boundary conditions were considered (Figure 3). The first one (Case A) considers that pallets are placed inside a chamber with uniform (99.5%) nitrogen concentration, whereas in the second one (Case B), the nitrogen concentration gradually increases from 78% to 99.5% [8]. Thus, the first scenario represents the shortest duration for low (1%) oxygen concentration to be reached at the pallet core, whereas the second one represents a realistic scenario (as already reported by Agrafioti et al. [8]).

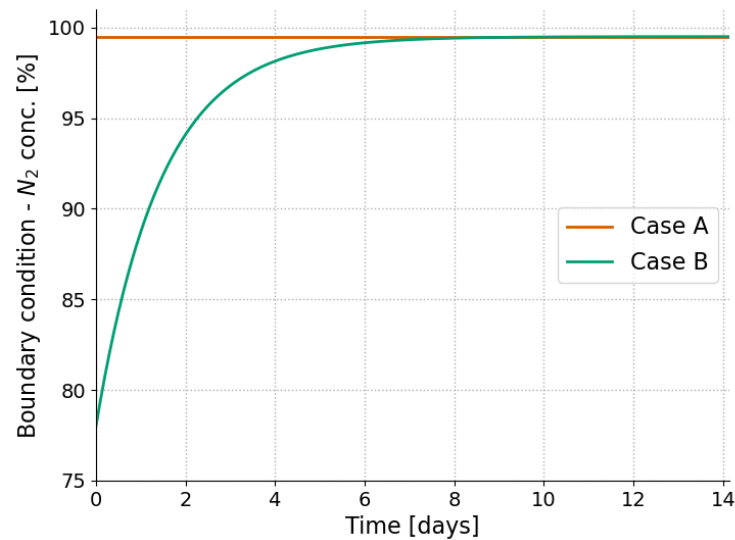


Figure 3. The two boundary conditions considered for this study for the chamber/pallet simulations.

3.1.1. Constant Boundary Condition (Case A)

The results for this scenario are displayed in Table 2 (under the column ‘Case A’). The average duration required for O₂ concentration to reach 1% is approximately 10.7 h. Among the individual items, walnuts (kernels) exhibit the shortest duration, predicted at 9.7 h, while prunes require the longest time at 11.5 h. This outcome aligns with expectations given the differing porosity levels, with prunes possessing the highest and lowest porosity values.

Table 2. Simulation results (time to reach 1% O₂) at the center of the pallet.

Product	Case A [h]	Case B (Total) [h]	Case B [h]
almonds (in-hull)	10.0	133.1	2.4
almonds (in-shell)	10.4	133.2	2.6
barley	11.0	133.4	2.7
cashew	10.8	133.4	2.7
corn	10.9	133.4	2.7
hazelnut (kernel)	11.1	133.4	2.8
pistachio (nut)	10.5	133.2	2.6
pistachio (kernel)	10.8	133.3	2.7
prunes	11.5	133.6	2.9
raisins	11.2	133.5	2.8
rice	10.5	133.2	2.6
soybean	11.3	133.5	2.8
walnut (shelled)	10.3	133.2	2.5
walnut (kernel)	9.7	133.0	2.3
wheat	11.0	133.4	2.8

By categorizing the agricultural products, it is evident that cereals (barley, corn, rice, wheat) reach the target oxygen concentration in the shortest time, with an average of approximately 10.75 h. Nuts (almonds (in-hull), almonds (in-shell), cashew, hazelnut (kernel), pistachio (nut), pistachio (kernel), walnut (shelled), walnut (kernel)), on the other hand, take a bit longer, with an average of approximately 10.15 h. Dried fruits, including prunes, raisins, and soybeans, require the most time on average, at approximately 11.33 h. This categorization shows that the product type plays a significant role in the time it takes to reach the desired oxygen concentration. Cereals, which are generally less porous, reach the target concentration more quickly than nuts and dried fruits, which have higher porosity levels.

3.1.2. Time Variable Boundary Condition (Case B)

The comprehensive time required for a 99% N₂ concentration, for the second boundary condition, to reach the center of the pallet is presented in Table 2 under the column “Case B (total)”. Additionally, the table indicates the time necessary to attain the desired concentration levels at the center of the pallet after the boundary condition has reached 99% N₂ (column “Case B”).

On average, in Case B (total), the treatment of agricultural products demands around 133.3 h (with a minimum of 133.0 h and a maximum of 133.6 h). No notable differences were observed between the nuts, grains and dried fruits categories. For column “Case B” specifically, the average duration is 2.7 h (ranging from a minimum of 2.3 h to a maximum of 2.9 h). Notably, similar to Case A, the extremities are attributed to the same products (walnuts and prunes, respectively). These findings indicate that, once the nitrogen concentration reaches 99%, the additional time required for the final 0.5% increase in nitrogen concentration is relatively consistent across different product categories and the variation among product types in this specific phase is minimal. It is evident that the primary factor influencing the duration is the shape of the boundary condition (the time taken to achieve 99% N₂ concentration), rather than the specific agricultural commodity being treated.

3.2. Silo

In this section, we examine a standard silo with a height of 30 m and a diameter of 10 m. A typical nitrogen generator has a flow capacity of 72 m³/hour, as cited in Athanassiou and Sakka [33]. The generator produces nitrogen with a purity of 99.5%. For this scenario, the simulation model predicts the vertical concentration profile of N₂ taking into account both the diffusion effects but also the forced N₂ flow (convection). Table 3 displays the time required for the N₂ concentration to reach 99% at three different heights: 10 m, 20 m, and the silo’s top at 30 m. It is evident that most agricultural products exhibit similar behavior, with average times of 13.5 h, 25.4 h, and 37.0 h for the respective locations.

Table 3. Simulation results (time to reach 1% O₂) at three positions in the silo. Height 30 m corresponds to the top of the silo.

Product	Height 10 m [h]	Height 20 m [h]	Height 30 m [h]
almonds (in-hull)	13.6	25.5	37.1
almonds (in-shell)	13.5	25.4	37.0
barley	13.5	25.3	36.9
cashew	13.5	25.4	36.9
corn	13.5	25.4	36.9
hazelnut (kernel)	13.5	25.3	36.9
pistachio (nut)	13.5	25.4	37.0
pistachio (kernel)	13.5	25.4	36.9
prunes	13.4	25.2	36.8
raisins	13.4	25.3	36.9
rice	13.5	25.4	37.0
soybean	13.4	25.3	36.8
walnut (shelled)	13.6	25.5	37.0
walnut (kernel)	13.6	25.6	37.2
wheat	13.5	25.3	36.9

Table 3 shows the required time for N₂ to reach 99% at 10 m, 20 m, and 30 m (top of the silo). It is clear that most of the agricultural products present the same behavior, i.e., 13.5 h, 25.4 h, and 37.0 h for the three locations. In contrast to the chamber scenario, the range of hours for each location is more constrained despite the greater distance. This phenomenon is due to the prevailing convection effects (induced flow from the generator) to a certain degree over diffusion effects, which are influenced by the commodity’s porosity.

The study of nitrogen distribution draws parallels to the analysis of thermoclines in hot water storage tanks during charging, as observed by Kaloudis et al. [34] and Kaloudis et al. [35].

Although the physical phenomena involve distinct fluid viscosities (nitrogen gas vs. water), the similarities in convection and diffusion make certain parameters applicable. For our study, the term “thermocline thickness” δ [35] is adapted to represent the diffusion layer’s thickness. Figure 4 illustrates that, at 12 h, the diffusion layer’s thickness was $\delta(12\text{ h}) = 4.49\text{ m}$, while at 24 h, $\delta(24\text{ h}) = 6.35\text{ m}$, consistent with the observations of Kaloudis et al. [34]. This alignment signifies the anticipated increase in the diffusion layer’s thickness over time.

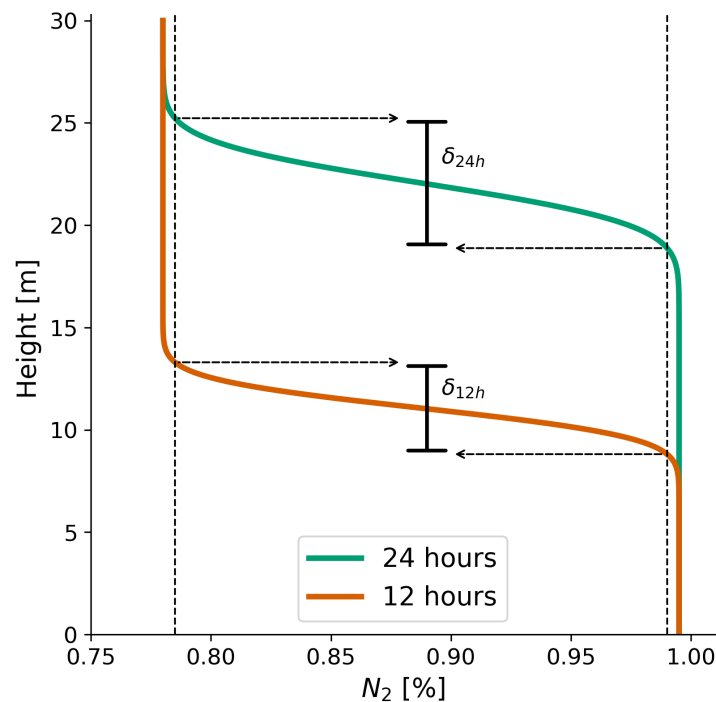


Figure 4. The distribution of nitrogen at two time instances.

4. Discussion

The utilization of computer simulations enabled a comprehensive exploration of the effects of modified atmospheres on insect control. The results presented insights into the dynamics of nitrogen distribution within various agricultural commodities, shedding light on the time required for oxygen concentration to decrease to desirable levels for pest suppression. Other examples of the successful use of computational methods in pest management include phosphine fumigation. In particular, Agrafioti et al. [13] have developed a computational fluid dynamics simulation model capable of investigating phosphine distribution in different storage structures. Their research aimed to correlate phosphine distribution patterns with insect mortality to improve precision fumigation strategies. They evaluated the accuracy of their models by comparing predictions with sensor data, highlighting their utility in predicting gas distribution and insect mortality during fumigation operations. They found that some of the factors that influence fumigant concentrations include environmental conditions and sorption by commodities, which is a common finding with the recent study.

In the case of chamber-contained pallets, the simulations provided valuable information regarding the duration needed for oxygen concentration to reach 1% within the core of the pallets. For instance, Sakka et al. [36] found that the increase of percentage of nitrogen in the atmosphere can be used with success against different life stages of the khapra beetle, *Trogoderma granarium* Everts (Coleoptera: Dermestidae), in commercial chambers, including different commodities such as plums, figs, and raisins. The current study considered both constant and time-variable boundary conditions, reflecting uniform nitrogen concentration and gradual nitrogen infusion, respectively. It was observed that the type of boundary

condition significantly influenced the time required for achieving the desired oxygen levels, with boundary shape playing a pivotal role. Moreover, variations in porosity among different commodities were found to impact the duration of oxygen reduction, corroborating the link between porous structure and gas diffusion. In the context of silos, the investigation delved into nitrogen distribution across varying heights within the silo. Convection effects, induced by nitrogen flow from generators, played a substantial role in addition to diffusion. The study demonstrated that, unlike the chamber scenario, the range of hours required for nitrogen concentration to reach specific levels in different heights of the silo was relatively constrained. This observation emphasized the dominance of convection effects, which contributed to a more consistent diffusion layer thickness over time.

Widespread adoption of modified atmospheres is largely dependent on cost considerations, mainly due to the need for specialized equipment that is often not available in conventional fumigation practices. In general, the application of nitrogen is more expensive than the dominant chemical control methods [3,31]. However, in the long term, the investment in nitrogen-based solutions for storage and processing facilities may be offset by the benefits, particularly the environmental attributes of this approach. A significant proportion of the cost is associated with the installation of the system, such as the siting of generators. Given the volatility of energy prices, it is imperative to re-evaluate all factors affecting the overall economics of this process.

Taking exposure time into account, Sakka et al. [37] studied adult populations of both phosphine-resistant and susceptible populations of the red flour beetle *Tribolium castaneum* (Herbst) (Coleoptera: Tenebrionidae), *O. surinamensis*, and *S. oryzae*. They conducted experiments in commercial nitrogen chambers, exposing the insects to 1% oxygen for various exposure times, including 2.5, 3, and 9 days. Their results showed complete mortality at 40 °C, but some survival was observed at 28 °C. Meanwhile, Agrafioti et al. [8] also investigated the effect of exposure time and temperature on *O. surinamensis* and *R. dominica*. They observed 100% mortality over a range of exposure times from 2.5 to 9 days and temperatures from 28 to 40 °C. Similar results were noted by Sakka et al. [36], in which complete control and suppression of progeny production were recorded for all life stages of *T. granarium* and adults of *T. castaneum* and *C. maculatus* at 40 °C for 2.5 days of exposure in commercial nitrogen chambers. It is worth noting, however, that in some of these experiments, exposure times exceeded 14 days, which is significantly longer than the typical exposure times associated with various conventional fumigants such as phosphine [38].

As highlighted in the introduction, the research area of computational modeling of modified atmospheres is relatively under-explored and this study represents a step towards filling this gap. However, it is important to recognize the limitations arising from the complexity and breadth of the subject matter, which makes it impractical to comprehensively address the full range of possibilities within this investigation. Future research should consider investigating additional factors that could potentially influence gas distribution, including but not limited to variations in temperature, humidity and pressure. Investigation of these variables would contribute to a deeper understanding of the dynamics involved in modified atmospheres. Furthermore, in order to improve the robustness of the computational model, it is recommended that subsequent studies incorporate a wider range of experimental data collected under different microenvironmental conditions, including variations in temperature and humidity. In addition, broadening the scope to include different boundary conditions, agricultural products, and storage structures (e.g., silos) would provide a more comprehensive validation of the simulation model. The inclusion of insect mortality models in future investigations could provide valuable insights, particularly in the visualization of specific areas of interest, such as the center of pallets. This addition would contribute to a more holistic understanding of the interactions between gas distribution and insect control.

5. Conclusions

This study contributes to the understanding of modified atmosphere techniques for insect control in stored agricultural commodities. The findings underscore the importance

of boundary conditions, commodity porosity, and convection effects in shaping the efficacy of modified atmosphere treatments. The advantages of the computational methodology outlined in the current research are its inherent configurability for a wide range of agricultural commodities, the incorporation of different structural geometries within storage facilities, and variable configurations of the nitrogen flow produced by the nitrogen generator. As an additional aspect, the purity of the nitrogen gas can be adjusted using the framework provided by the present method. Taken together, these imply that the computational methodology proposed in this scientific study has the capacity to be effectively applied to a wide variety of commercial nitrogen applications. Moving forward, this research can provide a basis for optimizing modified atmosphere strategies in real-world scenarios and provide practitioners and stakeholders with quantitative insights into the temporal and spatial dynamics of nitrogen distribution. Further investigations could explore additional factors that might influence gas distribution, such as temperature, humidity, and pressure variations. Moreover, experimental validation of the simulation results would enhance the accuracy of the predictions and strengthen the applicability of the proposed models to diverse agricultural settings. Overall, the study advances the knowledge surrounding modified atmospheres as a sustainable pest management strategy and provides a basis for refining and implementing these techniques in the agricultural industry.

Author Contributions: Conceptualization, E.K. and P.A.; methodology, E.K. and P.A.; software, E.K.; investigation, P.A.; writing—original draft preparation, E.K., P.A. and C.A.; writing—review and editing, E.K., P.A. and C.A. All authors have read and agreed to the published version of the manuscript.

Funding: This research is part of the project “Management of entomological infestations in the stored products by using innovative technologies” (Project code: KMP6-0081034) that is co-funded by Greece and the European Union by the Action “Investment Plans of Innovation” in Central Macedonia under the framework of the Operational Program “Central Macedonia 2021–2027”.

Data Availability Statement: No new data were created or analyzed in this study. Data sharing is not applicable to this article.

Conflicts of Interest: The authors declare no conflicts of interest.

References

1. Banks, H.; Annis, P.; Calderon, M.; Barkai-Golan, R. Comparative advantages of high CO₂ and low O₂ types of controlled atmospheres. In *Food Preservation by Modified Atmospheres*; Calderon, M.; Barkai-Golan, R., CRC Press: Boca Raton, FL, USA, 1990.
2. Calderon, M.; Barkai-Golan, R. *Food Preservation by Modified Atmospheres*; CRC Press: Boca Raton, FL, USA, 1990.
3. Navarro, S. The use of modified and controlled atmospheres for the disinfestation of stored products. *J. Pest Sci.* **2012**, *85*, 301–322. [[CrossRef](#)]
4. Athanassiou, C.G.; Arthur, F.H. *Recent Advances in Stored Product Protection*; Springer: Berlin/Heidelberg, Germany, 2018.
5. Ofuya, T.; Reichmuth, C. Control of two bruchid pests of stored grain legumes in a nitrogen atmosphere. *Crop Prot.* **1993**, *12*, 394–396. [[CrossRef](#)]
6. Athanassiou, C.G.; Chiou, A.; Rumbos, C.I.; Sotiroudas, V.; Sakka, M.; Nikolidaki, E.K.; Panagopoulou, E.A.; Kouvelas, A.; Katechaki, E.; Karathanos, V.T. Effect of nitrogen in combination with elevated temperatures on insects, microbes and organoleptic characteristics of stored currants. *J. Pest Sci.* **2016**, *90*, 557–567. [[CrossRef](#)]
7. Rumbos, C.I.; Sakka, M.K.; Vassilakos, T.N.; Athanassiou, C.G. Effect of Nitrogen on Stored-Product Insect Control at Industrial Scale. *Insects* **2023**, *14*, 518. [[CrossRef](#)] [[PubMed](#)]
8. Agrafioti, P.; Kaloudis, E.; Athanassiou, C.G. Utilizing low oxygen to mitigate resistance of stored product insects to phosphine. *J. Sci. Food Agric.* **2022**, *102*, 6080–6087. [[CrossRef](#)] [[PubMed](#)]
9. Guo, J.; Wei, X.; Du, X.; Ren, J.; Lü, E. Numerical simulation of liquid nitrogen injection in a container with controlled atmosphere. *Biosyst. Eng.* **2019**, *187*, 53–68. [[CrossRef](#)]
10. Silva, M.; Faroni, L.; Martins, M.; Sousa, A.; Bustos-Vanegas, J. CFD simulation of ozone gas flow for controlling *Sitophilus zeamais* in rice grains. *J. Stored Prod. Res.* **2020**, *88*, 101675. [[CrossRef](#)]
11. Carvalho, D.; Santos, I.; Vargas, G.; Martins, M.; Ferreira, A. Utilization of nitrogen gas for refrigeration and atmosphere modification in grain storage: A simulation study. In Proceedings of the 1st International Symposium on CFD Applications in Agriculture 1008, Valencia, Spain, 9–12 July 2012; pp. 127–132.
12. Pandiselvam, R.; Chandrasekar, V.; Thirupathi, V. Numerical simulation of ozone concentration profile and flow characteristics in paddy bulks. *Pest Manag. Sci.* **2017**, *73*, 1698–1702. [[CrossRef](#)]

13. Agrafioti, P.; Kaloudis, E.; Bantas, S.; Sotiroudas, V.; Athanassiou, C.G. Modeling the distribution of phosphine and insect mortality in cylindrical grain silos with Computational Fluid Dynamics: Validation with field trials. *Comput. Electron. Agric.* **2020**, *173*, 105383. [[CrossRef](#)]
14. Bird, R.; Stewart, W.; Lightfoot, E. *Transport Phenomena*, 2nd ed.; Wiley: Hoboken, NJ, USA, 2002.
15. Shen, L.; Chen, Z. Critical review of the impact of tortuosity on diffusion. *Chem. Eng. Sci.* **2007**, *62*, 3748–3755. [[CrossRef](#)]
16. Ghanbarian, B.; Hunt, A.G.; Ewing, R.P.; Sahimi, M. Tortuosity in Porous Media: A Critical Review. *Soil Sci. Soc. Am. J.* **2013**, *77*, 1461–1477. [[CrossRef](#)]
17. Barrande, M.; Bouchet, R.; Denoyel, R. Tortuosity of porous particles. *Anal. Chem.* **2007**, *79*, 9115–9121. [[CrossRef](#)] [[PubMed](#)]
18. Dingke, Z.; Fielke, J. Some physical properties of Australian Nonpareil almonds related to bulk storage. *Int. J. Agric. Biol. Eng.* **2014**, *7*, 116–122.
19. Tavakoli, M.; Tavakoli, H.; Rajabipour, A.; Ahmadi, H.; Gharib-Zahedi, S.M.T. Moisture-dependent physical properties of barley grains. *Int. J. Agric. Biol. Eng.* **2010**, *2*, 84–91.
20. Balasubramanian, D. PH—Postharvest Technology. *J. Agric. Eng. Res.* **2001**, *78*, 291–297. [[CrossRef](#)]
21. Seifi, M.R.; Alimardani, R. The Moisture Content Effect on Some Physical and Mechanical Properties of Corn (Sc 704). *J. Agric. Sci.* **2010**, *2*, 125. [[CrossRef](#)]
22. Aydin, C. PH—Postharvest Technology. *Biosyst. Eng.* **2002**, *82*, 297–303. [[CrossRef](#)]
23. Kashaninejad, M.; Mortazavi, A.; Safekordi, A.; Tabil, L. Some physical properties of Pistachio (*Pistacia vera* L.) nut and its kernel. *J. Food Eng.* **2006**, *72*, 30–38. [[CrossRef](#)]
24. Tsami, E.; Katsioti, M. Drying kinetics for some fruits: Predicting of porosity and color during dehydration. *Dry. Technol.* **2000**, *18*, 1559–1581. [[CrossRef](#)]
25. Karimi, N. Moisture-dependent physical properties of seedless and seeded raisin (*Vitis vinifera* L.) varieties. *Agron. Res. Mold.* **2015**, *161*, 5–16. [[CrossRef](#)]
26. Varnamkhasti, M.G.; Mobli, H.; Jafari, A.; Keyhani, A.; Soltanabadi, M.H.; Rafiee, S.; Kheiralipour, K. Some physical properties of rough rice (*Oryza sativa* L.) grain. *J. Cereal Sci.* **2008**, *47*, 496–501. [[CrossRef](#)]
27. Deshpande, S.; Bal, S.; Ojha, T. Physical Properties of Soybean. *J. Agric. Eng. Res.* **1993**, *56*, 89–98. [[CrossRef](#)]
28. Altuntaş, E.; Erkol, M.H. Physical properties of shelled and kernel walnuts as affected by the moisture content. *Czech J. Food Sci.* **2018**, *28*, 547–556. [[CrossRef](#)]
29. Karimi, M.; Kheiralipo, K.; Tabatabaee, A.; Khoubakht, G.; Naderi, M.; Heidarbeig, K. The Effect of Moisture Content on Physical Properties of Wheat. *Pak. J. Nutr.* **2008**, *8*, 90–95. [[CrossRef](#)]
30. Zoppou, C.; Knight, J.H. Analytical Solutions for Advection and Advection-Diffusion Equations with Spatially Variable Coefficients. *J. Hydraul. Eng.* **1997**, *123*, 144–148. [[CrossRef](#)]
31. Navarro, S.; Athanassiou, C.; Varnava, A.; Vroom, N.; Yiassoumis, D.; Leandrou, I.; Hadjioannou, S. Control of stored grain insects by using nitrogen in large concrete silos in Cyprus. In Proceedings of the 9th International Conference of Controlled Atmospheres and Fumigation in Stored Products, Antalya, Turkey, 15–19 October 2012; pp. 15–19.
32. Flat Pallets for Intercontinental Materials Handling—Principal Dimensions and Tolerances. Standard 6780:2003(EN); International Organization for Standardization: Geneva, Switzerland, 2004.
33. Athanassiou, C.G.; Sakka, M.K. Using Nitrogen for the Control of Stored Product Insects: One Single Application for Multiple Purposes. *Agrochemicals* **2022**, *1*, 22–28. [[CrossRef](#)]
34. Kaloudis, E.; Grigoriadis, D.; Papanicolaou, E.; Panidis, T. Large eddy simulations of turbulent mixed convection in the charging of a rectangular thermal storage tank. *Int. J. Heat Fluid Flow* **2013**, *44*, 776–791. [[CrossRef](#)]
35. Kaloudis, E.; Grigoriadis, D.; Papanicolaou, E. Numerical simulations of constant-influx gravity currents in confined spaces: Application to thermal storage tanks. *Int. J. Therm. Sci.* **2016**, *108*, 1–16. [[CrossRef](#)]
36. Sakka, M.K.; Gatzali, F.; Karathanos, V.; Athanassiou, C.G. Efficacy of low oxygen against *Trogoderma granarium* Everts, *Tribolium castaneum* (Herbst) and *Callosobruchus maculatus* (F.) in commercial applications. *J. Stored Prod. Res.* **2022**, *97*, 101968. [[CrossRef](#)]
37. Sakka, M.K.; Gatzali, F.; Karathanos, V.T.; Athanassiou, C.G. Effect of Nitrogen on Phosphine-Susceptible and -Resistant Populations of Stored Product Insects. *Insects* **2020**, *11*, 885. [[CrossRef](#)]
38. Agrafioti, P.; Sotiroudas, V.; Kaloudis, E.; Bantas, S.; Athanassiou, C.G. Real time monitoring of phosphine and insect mortality in different storage facilities. *J. Stored Prod. Res.* **2020**, *89*, 101726. [[CrossRef](#)]

Disclaimer/Publisher’s Note: The statements, opinions and data contained in all publications are solely those of the individual author(s) and contributor(s) and not of MDPI and/or the editor(s). MDPI and/or the editor(s) disclaim responsibility for any injury to people or property resulting from any ideas, methods, instructions or products referred to in the content.